Peertechz

Engineering Group

Journal of Civil Engineering and Environmental Sciences

DOI: http://dx.doi.org/10.17352/jcees

ISSN: 2455-488X

CC By

Kazuhiro Fujisaki*

Senior Academy of Kyushu Institute of Technology, Kitakyushu, Japan

Received: 24 September, 2018
Accepted: 03 October, 2018
Published: 04 October, 2018

***Corresponding author:** Kazuhiro Fujisaki, Senior Academy of Kyushu Institute of Technology, Kitakyushu, Japan, E-mail: fujisaki@msh.biglobe.ne.jp

Keywords: Chitosan; Flocculation window; Flocculation rate process; Microdose; Novel jar tester

https://www.peertechz.com

Research Article

Experimental study on flocculation performance of Chitosan-Based Flocculant using a Novel Jar Tester

Abstract

The effectiveness of chitosan as a flocculant was tested with a novel experimental apparatus. Using a newly developed flocculation tester, a large number of flocculation rate processes were measured. The novel jar tester included a photocoupler and switching timer. Mixing was paused for a period and the floc-settling velocity and residual turbidity were measured during this period. The relation between the turbidity of the supernatant (i.e., the residual turbidity) and chitosan dose was measured over a wide range of initial turbidities. The chitosan showed two windows for the optimum dose: (1) a dose close to that used with ordinary inorganic flocculants, at which the residual turbidity showed complicated behavior under the influence of various factors, and (2) an optimum dose in the order of 10^{-4} of the initial turbidity. The latter optimum-dose range is very narrow, and simple chargeneutralization plays an important role in the flocculation.

Introduction

Chitosan is a linear copolymer that is produced by deacetylation of chitin, which is the second-most abundant biopolymer in the world after cellulose. Owing to its unique properties, chitosan is used in many industrial applications [1]. Chitosan has also attracted significant amount of research attention as a promising coagulant and flocculant, (hereinafter, "flocculation" is used instead of "coagulation/flocculation", as well as "flocculant" instead of "coagulant/flocculant") owing to its environment friendly properties. Although many flocculation experiments have been conducted using chitosan and excellent reviews have been reported so far [1, 2], the mechanism of flocculation by chitosan has not been sufficiently clarified. This study aims to investigate the characteristics of chitosan when used as a flocculant. For this purpose, flocculation rate process and residual turbidity were measured with various chitosan doses over a wide range of initial turbidities. A novel flocculation tester was used for the measurement of these flocculation processes. This device includes photocouplers attached to both sides of a beaker. The flocculation experiments were conducted by intermittent mixing. When mixing was paused, the settling velocity of the floc and the residual turbidity of the solution were measured by light transmission. Flocculation windows, which indicate the effective range of flocculant doses, were demonstrated for a wide range of initial turbidities. In addition, the flocculation rate processes are also discussed.

Materials and Methods

Experimental setup

The experimental setup is shown in figure 1a. Photocouplers (I) and a switching timer (F) are attached to a conventional jar tester. The photocouplers are attached to both sides of the beaker for measuring the turbidity of the suspension (Figure 1b). Although several apparatuses for optical measurements of flocculation processes have been reported [3-7], they have all adopted suction and continuoussampling methods.

In the proposed study, residual turbidity was measured by pausing mixer and allowing flocs to settle in the beaker [8], which is a unique function of the novel jar tester. The photocouplers were composed of 680-nm-wavelength red

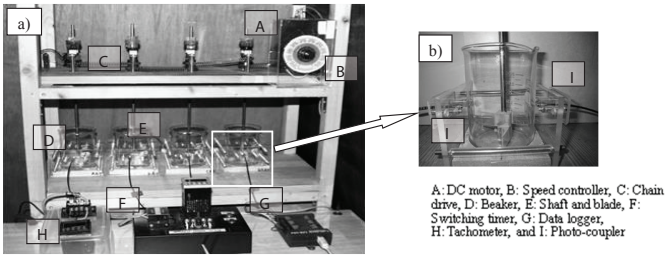

Figure 1: Experimental setup a) General assembly and b) close up of beaker with photo-coupler.

Citation: Fujisaki K (2018) Experimental study on flocculation performance of Chitosan-Based Flocculant using a Novel Jar Tester. J Civil Eng Environ Sci 4(2): 038-043. DOI: http://doi.org/10.17352/2455-488X.000026

light-emitting diode (LED) lasers and fiber-type analog optical sensors (F71RAN Takenaka Denshi Co., Ltd., Japan).

Calibration curve and sample powder

Figure 2 shows the relationship between the solids concentration, or turbidity, and the output voltage of the turbidity meter developed for these tests. The vertical and horizontal axes represent the concentration (mg/L) of grade-1 kaolin powder introduced to the suspension and the output voltage of the turbidity-meter sensor, respectively. Reagent-grade kaolin powder was not used in the flocculation experiment, because it is expensive and because we had to conduct a very large number of trials. However, the solid particles/flocs concentrations could all be expressed as equivalent kaolin particle concentrations using this calibration curve. Figure 2 shows that it is possible to measure particle concentrations from 1 to 1000 mg/L using this device.

White clay powder for painting ("Shiroetuchi" Asaoka Ceramic Material Co., Ltd., Japan), with properties like those of standard kaolin powder, was used in this study. The ignition loss of this powder is 12.5%, and the main constituents are 47.6% SiO_2, 38.5% Al_2O_3, 0.52% Fe_2O_3, 0.05% CaO, 0.22% MgO, 0.42% K_2O, 0.11% Na_2O, 0.28% TiO_2. The settling-velocity distribution of the sample powder is shown in figure 3. The vertical axis of figure 3, cumulative finer, is the mass-ratio of the particles moving slower than the settling velocity on the horizontal axis to the total particles in the suspension.

Flocculant and other experimental conditions

The flocculant tested in this study was a commercially available chitosan-based flocculant (FUJI Clean

KT-250, Fuji Engineering Co., Ltd., Japan). Hereinafter, "chitosan" is used in place of "chitosan-based flocculant". It has been reported that the molecular weight of this chitosan powder flocculant is on the order of 10^6 and that its degree of deacetylation is about 60%. Household well water was used, with temperature in the range of 15–25 and pH = 6.5, respectively.

The mixing conditions were standardized as follows: strong mixing at 250 rpm (G = 1150 s^{-1}) for 4 min, performed twice (total 8 min = 480 s) and, after that, slow mixing at 60 rpm (G = 135 s^{-1}). The photocoupler was located 2.4 cm below the water surface. A total of 250 mL suspension containing the sample powder and flocculant was introduced to the 300-mL beaker. The suspension is initially stirred for 30 minutes. The mixing and pausing steps both lasted for 4 min. The residual turbidity is defined as the turbidity of supernatant containing particles whose settling velocities below 0.01 cm/s (i.e., 2.4 cm/240 s). The output voltage corresponding to transmitted light was recorded continuously on a computer via data-logger.

Results and Discussion

Examples of experimental results

Figure 4 plots the temporal variation in the suspension turbidity. The horizontal and vertical axes represent the time (s) elapsed from the start and the residual turbidity of the suspension (mg/L), as measured 2.4 cm below the suspension surface. During the mixing periods, the turbidities were high and varied little, whereas during the intermittent pauses the floc concentration rapidly declined due to settling. For the analysis of flocculation processes, the measured results shown in figure 4 can be divided into two parts, periods for mixing (Figure 5) and still conditions (Figure 6).

Figure 5 excludes the settling periods shown in figure 4. Thus, the horizontal axis in figure 5 represents the net mixing time. The gray curves with origins shifted by 200 s in figure 5 represent the results from continuous-mixing trials, which had no pauses. Since the two curves and their residual turbidity mostly match, the effectiveness of the intermittent mixing method is confirmed.

Figure 6 shows only the data from the intermittent pauses. With increasing mixing time, the flocs grow, so the settling speed increases, which increases the slopes of these curves. The distribution of flocsettling velocities can be obtained by differentiating these curves. Also, by connecting the tops of these curves, we find rate at which the residual turbidity decreased, as discussed below.

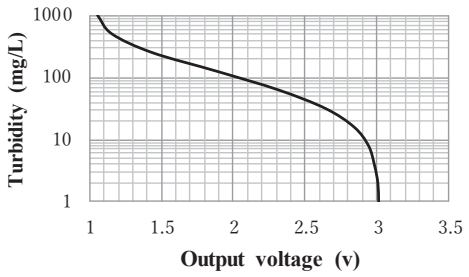

Figure 2: Reference curve.

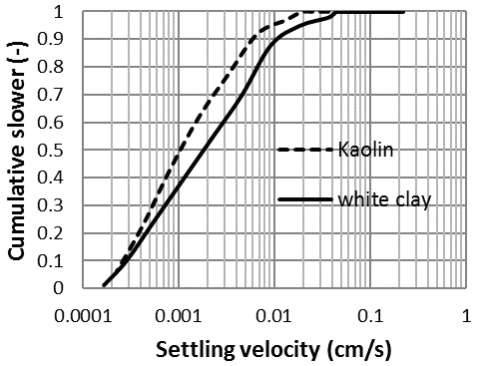

Figure 3: Settling velocity distribution of whiteclay sample and kaolin powder.

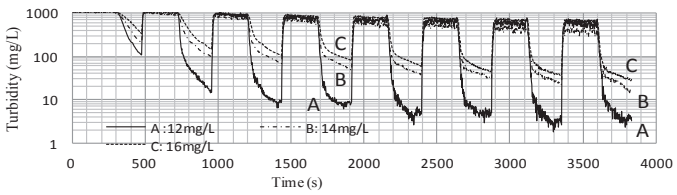

Figure 4: Example of variation in residual turbidity over time.

Citation: Fujisaki K (2018) Experimental study on flocculation performance of Chitosan-Based Flocculant using a Novel Jar Tester. J Civil Eng Environ Sci 4(2): 038-043. DOI: http://doi.org/10.17352/2455-488X.000026

Ordinary–dose flocculation window

For various initial turbidities, the influence of chitosan dose on residual turbidity is plotted in figure 7. The horizontal axis represents the chitosan dose (mg/L) and the vertical axis represents the residual turbidity (turbidity of the supernatant). The solid and broken lines indicate residual turbidities measured after 32 min and 64 min of mixing. These mixing durations were chosen as temporary standards for short- and long-term mixing, respectively, to allow comparison of flocculation processes measured under identical mixing conditions.

Usually, the central regions of such windows show the optimal dose, since flocculation decreases with either under- or over-dosing. Thus, the windows usually show U-shaped residual turbidity curves. However, in this experiment, as shown in figure 7, the curves were not monotonic. When the dose was increased above the optimal dose, flocculation deteriorated [1-3]. However, further increasing the dose promotes flocculation [9].

Chitosan flocculant seems to have the unique characteristic that a waveform appears in the flocculationwindow curve. In addition, these windows show the unique features corresponding to each initial turbidity. For the initial turbidity 500 mg/L (Figure 7a), if the dose range is 20 mg/L or more (except near 50 mg/L), the two curves show similar shapes, which suggests that the flocculation performance is similar in this dose range. With mixing for 32 min, a waveform clearly appears in the windows of 1000 mg/L (Figure 7b) and 6000 mg/l (Figure 7d) and the two curves show similar trends. On the contrary, in the 64-min mixing window shown in figure 7b and 7d, the curves show quite different shapes. In addition, in the case of 2000 mg/L (Figure 7c), the window waveform resembles the 500 mg/L case (Figure 7a) more than the others (Figure 7b,7d). Since various factors influence the adsorption of chitosan on the particle surfaces, these waveforms provide useful initial data for a detailed study of the complex mechanisms of flocculation using chitosan.

Small-dose flocculation window

Figure 8 shows the influence of a small dose of chitosan on residual turbidity figure 8. Is an expansion version of the small-dose region of figure 7, with the horizontal axis expanded on a logarithmic scale. Clearly, the chitosan strongly encourages flocculation, even at very small doses figure 8. Shows that the optimal dose range is very narrow and the residual turbidity is less than in the ordinary dose case (Figure 7). Furthermore, the flocculation rate is also very high. In figure 8, the flocculation is nearly complete after 32 min of mixing.

When normalized values are compared, meaning we convert both axes to relative values by dividing them by the respective initial turbidity, the four curves resemble each other (Figure 9), indicating that the flocculation mechanisms are similar in this very-small-dose region. The results also indicate that the value of the optimum relative dose is $(0.2–2) \times 10^{-4}$.

The following mechanisms have been considered to explain flocculation by chitosan: simple charge neutralization, charge patching, adsorption, bridging, and sweeping [1,2,10,11]. In the case of the microdose (Figure 8), charge neutralization seems predominant, since the optimum dose is proportional to the initial turbidity [2,15], while at higher doses, e.g., larger than 1–10 mg/L (Figure 7), other mechanisms seem to be involved in a complicated manner. Chitosan has been reported to have a

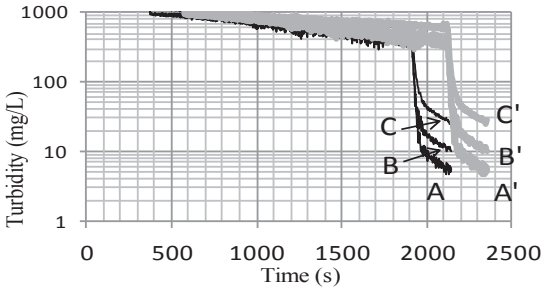

Figure 5: Final stage of flocculation.

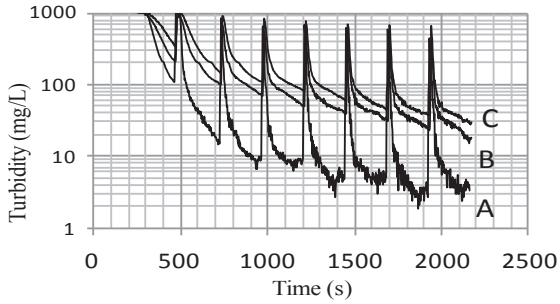

Figure 6: Time variation of settling velocity.

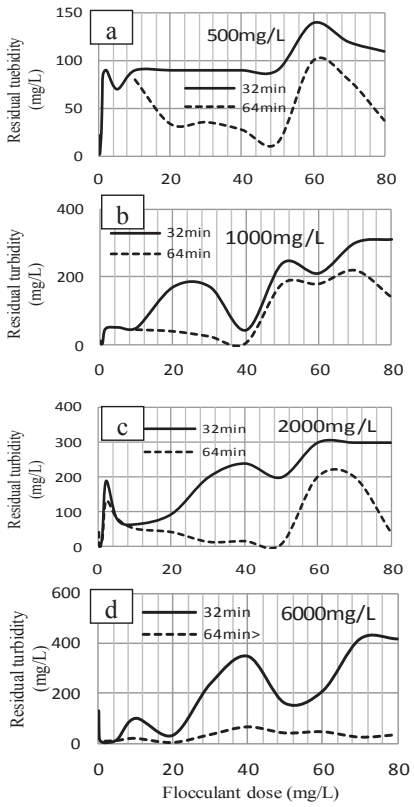

Figure 7: Flocculation windows –ordinary dose-.

Citation: Fujisaki K (2018) Experimental study on flocculation performance of Chitosan-Based Flocculant using a Novel Jar Tester. J Civil Eng Environ Sci 4(2): 038-043. DOI: http://doi.org/10.17352/2455-488X.000026

highly efficient flocculation effect even at small doses [1, 9-10, 12-14]. The experimental results shown in Figure 8 confirm the results of previous research.

To check the influence of beaker contamination, a blank experiment with no chitosan dose was performed, and confirmed the validity of the present experimental results.

Flocculation rate processes

The flocculation rate processes with different doses are compared in figure 10. The horizontal and vertical axes represent the net mixing time and the residual turbidity, respectively. The initial turbidity was 1000 mg/L in all trials. Clearly, the variation in flocculation rate processes depended on the dose. For example, in the $_{0.01\ mg}$/L dose case, flocculation ends after only 12 min (720 s) of mixing. On the other hand, when the dose was 0.1 mg/L, flocks also rapidly grew, but then repeated cycles of breakage and reflocculation occurred. At other doses such as 0.5, 20, and 40 mg/L, the flocculation seemed to have paused despite continuous mixing. To investigate which phenomena occurred during this "pauses", simultaneous measurements of chitosan adsorption and the zeta potential on the particle surfaces are necessary.

To facilitate a more-detailed discussion of the flocculation rate processes shown in figure 10, the timevariations of floc-settling velocity distributions are shown in figure 11. In the early stages of flocculation, very small, relatively uniform-size flocs were produced with all three doses. For the 0.1 mg/L dose, flocculation was almost finished after only a very short mixing period, 480 s. On the other hand, for the 0.5 mg/L dose, the flocs mixed for 960–1680 s did not significantly grow during mixing, while for the 40 mg/L dose, the flocs mixed for a time range 1440–2880 s showed remarkable growth during mixing. These findings are consistent with the corresponding flocculation rate processes shown in figure 10. For the 0.1 and 0.5 mg/L dose, the floc-settling velocities were around 0.06 cm/s. For the 40 mg/L dose, despite relatively high floc-settling velocity, 0.3 cm/s, the residual turbidity was rather high. In this case, the floc-size distribution is broad, so small flocs remained in the suspension for a long time.

Figure 12 shows the flocculation rate processes for various initial turbidities. The horizontal axis represents the net mixing time, and the vertical axis represents the relative turbidity, that is, the residual turbidity divided by the initial turbidity. The caption, for example, "500:0.1" means that the initial turbidity was 500 mg/L and chitosan flocculant dose was 0.1 mg/L. The same notation is used for the captions in figure 13. In figure 12a and 12b, for each initial turbidity, the dose that shows normal or relatively good flocculation performance is selected. For large doses (Figure 12a), all the curves show a "preparatory or pause period," in which the flocculation speed slows to near zero; after this interval, flocculation resumes. Although the duration of this period varies depending on the initial turbidity, the pauses tended to begin around 200 s.

For small doses (Figure 12b), the relative residual turbidities decreased to 1/1000 of the initial turbidities within 600 s of mixing, except when the initial turbidity was 500 mg/L.

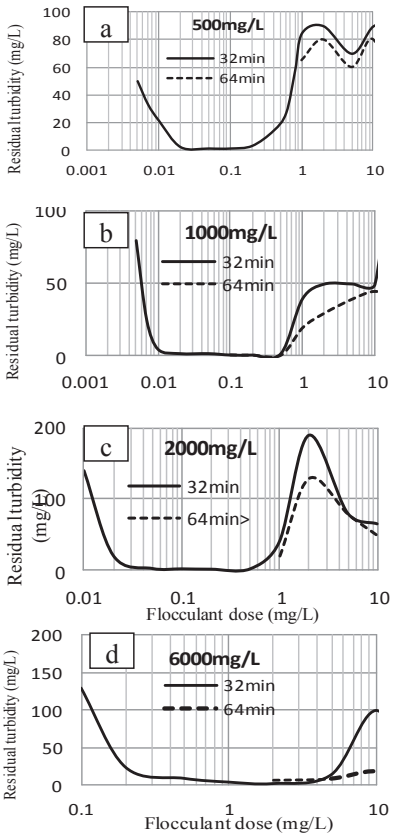

Figure 8: Flocculation window –small dose-.

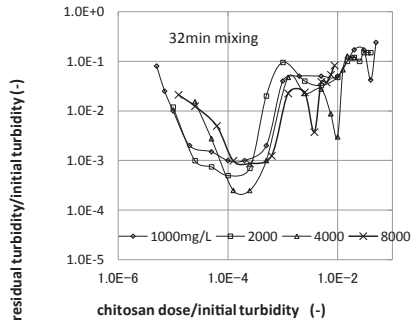

Figure 9: Comparison of windows with normalized scale.

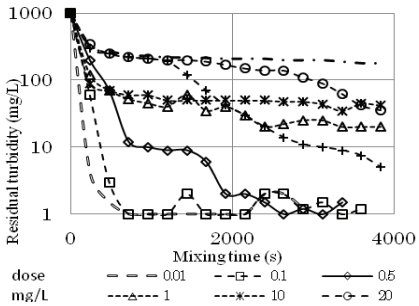

Figure 10: Flocculation rate process.

This rapid decrease indicates that the chitosan encourages flocculation remarkably well, even at small doses. In addition, some of the curves showed similar shapes, suggesting that similar phenomena took place during flocculation.

Citation: Fujisaki K (2018) Experimental study on flocculation performance of Chitosan-Based Flocculant using a Novel Jar Tester. J Civil Eng Environ Sci 4(2): 038-043. DOI: http://doi.org/10.17352/2455-488X.000026

Furthermore, for up to about 500 s of mixing, the curves were also close to linear, meaning that the flocculation kinetics can be approximated as a first-order chemical reaction.

Figure 13, shows the floc-settling velocity distributions for various initial turbidities figure 13a. Compares the floc-settling velocities achieved with small chitosan doses and for the short mixing time of 480 s. When the initial turbidity was relatively low (i.e., in the range 500–1000 mg/L), although the floc sizes were nearly uniform, the settling velocities were slow since the floc size is also small. Figure 13b, compares the settling velocities achieved with a large chitosan dose and long mixing time of 1920 s. In this case, the settling-velocity distributions were broader and the settling velocities were several times higher with the large doses than they were with the small ones. It should be noted that this figure is presented only for the sake of comparison. Clearly, some of the samples mixed for 1920 s were still flocculating at the end of the tests. In figures 10–13, the flocculation rate processes under various conditions are depicted. The characteristics of chitosan flocculation are clearly shown in these figures. Therefore, the present experimental data provides important information for the advanced analysis of flocculation mechanism with chitosan.

The variance in the measured turbidities was generally within 5%, the data, however, sometimes showed large scattering in the dose range where the curves of flocculation window had steep slopes. A detailed study is currently ongoing to understand this process better.

Conclusions

This study demonstrates that chitosan encourages flocculation via different mechanisms depending on the dose. The optimum doses for chitosan flocculant fall into two optimal windows. At very small doses, a microdose, on the order of 10^{-4} of the initial turbidity and the second was approximately 10^{-3} of the initial turbidity, which is on the same scale as the dose used for usual inorganic flocculants. In this normal-dose regime, the residual turbidity curves are not U-shaped, but fluctuate with increasing chitosan dose. In the microdose window, on the other hand, flocculation proceeds quickly and the residual turbidity is low. These unique results reflect inherent properties of biopolymer flocculant chitosan. Thus, the above results may prove useful in further studies on flocculation mechanisms of chitosan related flocculants. In addition, the novel experimental photocoupler apparatus proves to be a useful and inexpensive tool for flocculation studies.

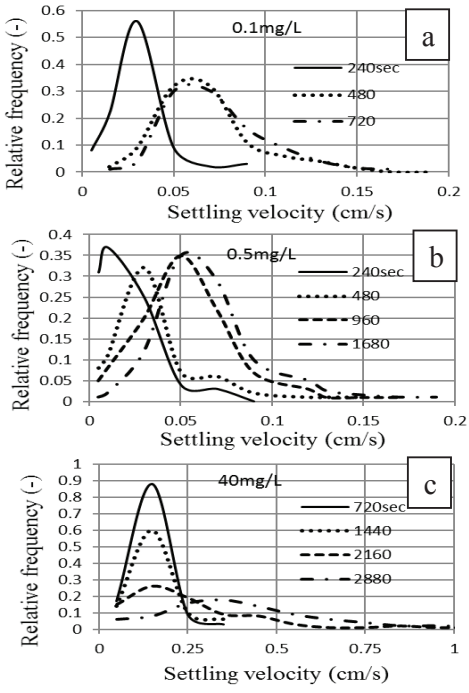

Figure 11: Time variation of floc settling.

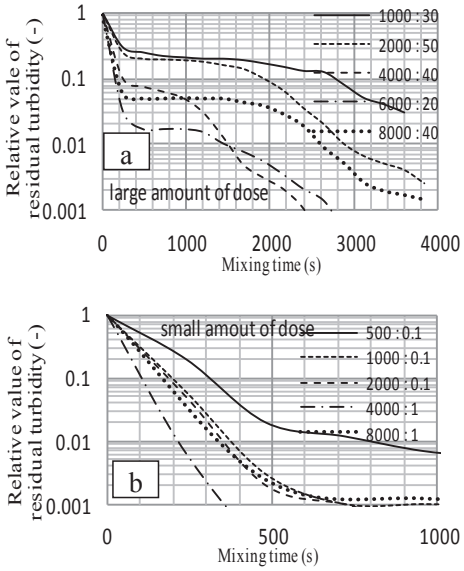

Figure 12: Flocculation rate process.

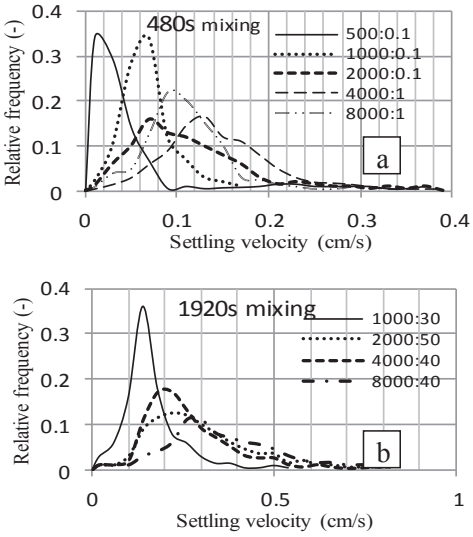

Figure 13: Time variations of floc settling velocity.

Acknowledgements

The chitosan flocculant used in these tests was donated by Fuji Engineering Co. Ltd, for which the author is grateful.

Citation: Fujisaki K (2018) Experimental study on flocculation performance of Chitosan-Based Flocculant using a Novel Jar Tester. J Civil Eng Environ Sci 4(2): 038-043. DOI: http://doi.org/10.17352/2455-488X.000026

References

1. Renault F, Sancey B, Badot P M, Crini G (2009) Chitosan for coagulation/ flocculation processes—An ecofriendly approach. European Polymer Journal. 45:1337–1348. Link: https://goo.gl/h9TE9A

2. Yang R, Li H, Huang M, Yang H, Li A (2016) A review on chitosan-based flocculants and their applications in water treatment. Water Research. 95:59–89. Link: https://goo.gl/gzPfEu

3. Huang C, Chen GS (1996) Use of the fiber-optical monitor in evaluating the state of flocculation. Water Research. 30: 2723–2727. Link: https://goo.gl/84AMHH

4. Gregory J (2004) Monitoring floc formation and breakage. Water Science and Technology. 50: 163170. Link: https://goo.gl/egb7vE

5. Gregory J (2009) Optical monitoring of particle aggregates. Journal of Environmental Science. 21: 2–7, 2009. Link: https://goo.gl/vxLf8r

6. Yang Z, Yang H, Jiang Z, Huang X, Li H, et al. (2013) A new method for calculation of flocculation kinetics combining Smoluchowski model with fractal theory. Colloid and Surfaces A: Physicochem. Eng. Aspects. 423 : 11-19. Link: https://goo.gl/T5NWKd

7. Zhang Z, Liu D, Hu D, Li D, Ren X, et al. (2013) Chen Y, Luan Z: Effects of slow mixing on the Coagulation Performance of Polyaluminum Chloride. Energy Resources and Environmental Technology, Chinese Journal of Chemical Engineering. 21: 318-323. Link: https://goo.gl/hZhKbd

8. Fujisaki K (2015) Comparison of Flocculation Properties with use of a new flocculation tester, Modern Environmental Science and Engineering. 1: 304–310.

9. Roussy J, Van Vooren M, Dempsey BA, Guibal, E (2005) Influence of chitosan characteristics on the coagulation and the flocculation of bentonite suspensions. Water Research. 39: 3247–3258. Link: https://goo.gl/yzGWPd

10. Guibal E, Van Vooren M, Dempsey BA, Roussy J (2006) A review of the use of chitosan for the removal of particulate and dissolved contaminants. Separation Science Technology. 41: 2487–2514. Link: https://goo.gl/zmtmzd

11. Guibal E, Roussy J (2007) Coagulation and flocculation of dye-containing solutions using a biopolymer (Chitosan). Research & Functional Polymers. 67: 33-42. Link: https://goo.gl/5baKBK

12. Fabris R, Chow CW, Drikas M (2010) Evaluation of chitosan as a natural coagulant for drinking water treatment. Water Science Technology. 61: 2119–2128. Link: https://goo.gl/bBNhuL

13. Li J, Jiao S, Zhong L, Pan J, Ma Q (2013) Optimizing coagulation and flocculation process for kaolinite suspension with chitosan. Colloid and Surfaces A: Physicochemical and Engineering Aspects. 428: 100-110. Link: https://goo.gl/p3wbQG

14. Yang Z, Li H, Yan H, Wu H, Yang H, et al. (2014) Evaluation of a novel chitosan-based flocculant with high flocculation performance, low toxicity and good floc properties. Journal of Hazardous Materials. 276: 480–488. Link: https://goo.gl/PR9Ect

15. Yang Z, Shang Y, Lu Y, Chen Y, Huang X, et al. (2011) Flocculation properties of biodegradable amphoteric chitosan-based flocculants. Chemical Engineering Journal. 172: 287–295. Link: https://goo.gl/BHtUpZ

Citation: Fujisaki K (2018) Experimental study on flocculation performance of Chitosan-Based Flocculant using a Novel Jar Tester. J Civil Eng Environ Sci 4(2): 038-043. DOI: http://doi.org/10.17352/2455-488X.000026